Code:1-121

Continuum mechanics beam theory for determining soil-structure interaction uncertainties and their effects on building vulnerability functions in subsidence regions

Ali. Saeidi[1], Olivier. Deck[2], Thierry.Verdel[3]

1-Centre d'études sur les ressources minérales, Université du Québec à Chicoutimi, ali_saeidi@uqac.ca
2,3-Université de Lorraine, GeoRessources, UMR 7359, Nancy, F-54042, France

ABSTRACT

The extraction of ore and minerals by underground mining or other underground workings often cause ground subsidence phenomena. In urban regions, these phenomena may induce small to severe damage to buildings. We have developed vulnerability functions for determining damage to building in subsidence regions. The methodology uses Monte Carlo simulations, and existing analytical methods based on the beam theory for the evaluation of damage in the subsidence area. It allows taking into account uncertainties both on the geometrical and mechanical parameters of buildings, and on the phenomena of soil structure interaction for analytical methods. This paper focuses on uncertainties on soil-structure interaction. The determination of damage with analytical methods requires values of the horizontal strain and the deflection transmitted to buildings. But the available geotechnical parameters are the horizontal ground strain and the ground curvature; soil structure interaction parameters are then required to determine how these geotechnical strains are transmitted to buildings. The value of these later parameters are dependent on several factors, such as the soil and the building rigidity, the building type, the mine or tunnel depth, the localisation of building in a subsidence basin. All of these factors increase the uncertainties in building vulnerability functions, and must be considered in the development of these functions. We observed that low values of ground curvature coefficient (K_Δ) lead to a flattening of the vulnerability curve (low vulnerability), and that low values of horizontal strain soil-structure interaction coefficient ($K\varepsilon$) lead to a shift of the vulnerability curve to the right (reduced vulnerability). Finally, it also appears that the building vulnerability curves are more sensitive to K_Δ values than to $K\varepsilon$ values.

1 INTRODUCTION

Ore and mineral extraction via underground mining may induce ground subsidence phenomena. These phenomena lead to horizontal and vertical ground movements, which consequently lead to deformations and damage in buildings of undermined urban regions (Figure 1). The maximum vertical displacement occurs in the centre of the subsidence area and may reach several meters. This displacement is accompanied by horizontal ground strains, ground curvature, and slope, the three types of movement that load structures and cause structural damage (Saeidi et al. 2013).

Figure 1 described the main dimensions and characteristics of a mining subsidence for a longwall mine. Depending on the subsidence kinetic, location of buildings in a subsidence is time dependent. A building may be in the traction and hogging area when the subsidence starts and be in the compression and sagging area when the subsidence stops. When mining subsidence is accidental, the kinetic is generally uncertain and the final location of the building is considered to assess the lower bound of the ground movements in the building vicinity. Two parameters are used to quantify the subsidence intensity in relation to the building damage: the horizontal ground strain that is associated with the horizontal load of the buildings, and the ground curvature that is associated with the deflection of the buildings.

The assessment of building damage in mining subsidence hazard areas can be performed using three types of method: empirical, analytical and numerical methods. Empirical methods are based on the analysis of a large number of observations of damage to buildings. The simplest method is threshold values of the ground displacements (Skempton and MacDonald, 1956). The

National Coal Board method (NCB, 1975) is one of the most famous, and it addresses the damage assessment with the building length and the horizontal ground strain. Analytical methods are based on the use of beam theory (Timoshenko, 1957) to assess the global behaviour of a building in relation to its geometry and mechanical properties. The first method was developed by Burland and Wroth (1974), and many extensions are now available (Boone, 1996; Finno et al. 2005). Numerical methods are mostly used for the prediction of ground movements (Melis et al., 2002, and Coulthard and Dutton 1998), the study of soil structure interaction and the assessment of the transmitted ground movements (Selby, 1999, Franzius et al. 2006, Son and Cording 2005, and Burd, 2000). But very few studies address the question of the damage assessment with numerical methods.

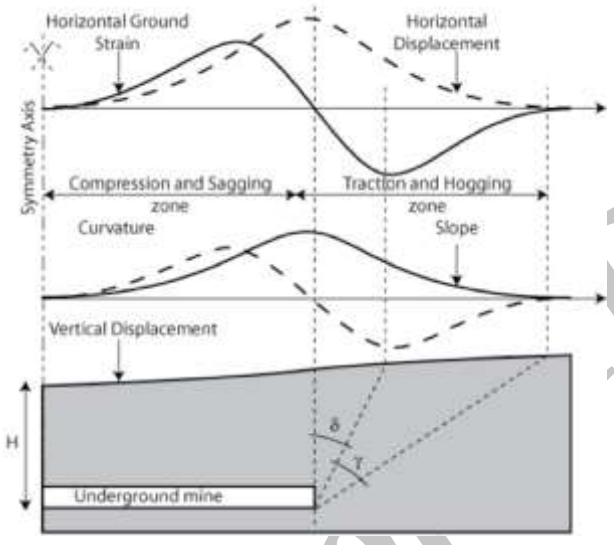

Figure 1. Description of the main characteristics of mining subsidence and associated consequences (Saeidi et al. 2009).

This paper first explains the methods of development of vulnerability functions in subsidence areas. This resulting algorithm is then used for evaluating the effects of several values of the soil-structure coefficient on building damage in these areas.

2 METHODOLOGY FOR THE DEVELOPMENT OF ANALYTICAL VULNERABILITY FUNCTIONS IN A SUBSIDENCE AREA

The methodology adopted in this study to develop vulnerability and fragility curves is based on the damage assessment of a set of theoretical buildings whose characteristics are consistent with a particular building type, but are also variable in order to take into account both the variability of the building type and the uncertainty in parameter values.

The method is based on four steps, the first one consisting in a preliminary selection of damage scale, of an intensity criterion and an analytical method for the building damage evaluation. A five-level damage scale is selected, and the intensity criterion is the horizontal ground strain parameter ε_{ground}. The second step consists of defining a building typology and selecting the representative characteristics of each type.

For each type, the third step consists of simulating a database of 1000 virtual buildings whose characteristics (e.g., height, length, materials, and mechanical properties) are consistent with the studied building type.

The fourth step consists of evaluating the damage of the 1000 simulated buildings for one value of the intensity criterion and counting the number of buildings into each damage class. The results may then be used to plot a set of points for both the fragility curve (probability of reaching or exceeding a given damage class) and the vulnerability curve (mean damage). Finally, by repeating this step for all the values of the horizontal ground strain, both the vulnerability and the fragility curves can be drawn.

3 ANALYTICAL METHODS FOR BUILDING DAMAGE EVALUATION

The first analytical method for building damage assessment was developed by Burland and Wroth (1974), and several extensions are now available (Boscardin and Cording, 1989, Boone, 1996, Burland, 1995, Finno et al. 2005). In these methods, masonry buildings are modelled using an isotropic and elastic beam with two supports, loaded by a central or uniformly distributed load. A deflection Δ is imposed on the beam to model the ground curvature that corresponds to the bending effect of the subsidence on the building. The maximum tensile strains due to bending and shear deformations are then calculated and compared with the values of the critical tensile strains for the determination of the damage class. All of the current analytical methods use five damage classes, and Table 1 gives the five damage classes defined by Burland (1995) and Boscardin and Cording (1989).

Differences between these methods concern the modelling of the subsidence effect, the loading distribution (building weight), the location of the neutral axis, the building type and the imposed relationships between the mechanical parameters.

3.1 Burland's method

As explained in the previous section, Burland's method considers the building as an isotropic beam with dimension L for the length, H for the height and with a unit thickness. The beam can be affected both by the horizontal ground strain and the ground curvature. A transmitted vertical deflection Δ is imposed at the centre of the beam to model the effect of the ground curvature, and a uniform transmitted horizontal strain ε_h is imposed to model the effect of the horizontal ground strain.

Based on the theory of Timoshenko (1957), Burland and Wroth (1974) identified two critical sections in the beam where maximal tensile strains occur; the half span section and the edge section. In these two sections, the maximal tensile strain must be calculated in order to allow a comparison to threshold values associated with different damage classes.

The relationships between Δ and the maximum tensile strain ε_b in the half-span critical section, or the maximal diagonal tensile strain ε_d in the edge section, are calculated according to Equations 1 and 2 (Burland 1995), where y is the distance between the neutral axis and the lower fibre of the beam.

$$\frac{\Delta}{L} = \left[\frac{5 \cdot L}{48 \cdot y} + \frac{3 \cdot I}{2 \cdot y \cdot L \cdot H} \cdot \frac{E}{G}\right] \varepsilon_b \qquad [1]$$

$$\frac{\Delta}{L} = \left[\frac{1}{2} + \frac{5H \cdot L^2 G}{144 \cdot E \cdot I}\right] \varepsilon_d \qquad [2]$$

The effect of the uniform horizontal transmitted strain ε_h, may then be added in order to calculate the maximal value of the principal tensile strain in the two critical sections.

In the half span critical section, both Δ and ε_h induce principal horizontal tensile strains. The maximal tensile strain ε_{bmax} is then estimated as the sum of these two principal tensile strains (Eq. 3):

$$\varepsilon_{b\max} = \varepsilon_b + \varepsilon_h \qquad [3]$$

In the edge critical section, Δ induces vertical shear stresses and ultimately a diagonal principal tensile strain, while ε_h induces a horizontal principal tensile strain. The maximal tensile strain ε_{dmax} is then evaluated using Mohr's circle of strain (Eq. 4, Burland 1995).

$$\varepsilon_{d\max} = \varepsilon_h\left(\frac{1-\nu}{2}\right) \pm \sqrt{\varepsilon_h^2\left(\frac{1+\nu}{2}\right)^2 + \varepsilon_d^2} \qquad [4]$$

For an isotropic beam, ν can be replaced by E/2G–1 with the E/G ratio between 0.5 and 3. By substituting the values of ε_b in Equation 1 into Equation 3, and ε_d in Equation 2 into Equation 4, the relationship between the relative deflection parameter (Δ/L), the transmitted horizontal strain (ε_h) and other building parameters is calculated for the two critical sections (Equation 5).

$$\begin{cases} \frac{\Delta}{L} = \left[\frac{5 \cdot L}{48 \cdot y} + \frac{3 \cdot I}{2y \cdot L \cdot H} \cdot \frac{E}{G}\right](\varepsilon_{b\max} - \varepsilon_h) & \text{Mid-span critical section} \\ \frac{\Delta}{L} = \left[\frac{1}{2} + \frac{5H \cdot L^2 G}{144 I \cdot E}\right] \sqrt{\left[\varepsilon_{d\max} - \varepsilon_h\left(1 - \frac{E}{4G}\right)\right]^2 - \varepsilon_h^2\left(\frac{E}{4G}\right)^2} & \text{Edge critical section} \end{cases} \qquad [5]$$

Burland et al. (1977) defined the concept of limiting tensile strain ε_{lim} that must be compared to the maximal tensile strains ε_{bmax} and ε_{dmax} to define the threshold value of the maximal tensile strain before damage occurs. Like Boscardin and Cording (1989), Burland (1995) defined different threshold values for different damage levels according to Table 1, and they considered these values for a large quantity of buildings. Most of the analytical methods use these threshold values to assess the building damage.

Table 1. Threshold values of the limiting tensile strain ε_{lim} associated with the five damage classes (Boscardin and Cording 1989).

Damage class		**Limiting tensile strain (ε_{lim})%**
D_0	Negligible	0-0.05
D_1	Very slight	0.05-0.075
D_2	Slight	0.075-0.15
D_3	Moderate	0.15-0.3
D_4 and D_5	Severe to Very Severe	>0.3

The two relations in Equation 5 are usually used to plot the $\Delta/(L.\varepsilon_{lim})$ ratio versus the L/H ratio for given values of the building mechanical properties, and the uniform horizontal transmitted strain ε_h. Figure 2 shows a result for the case where ε_h is set equal to 0, the E/G ratio is 2.6 (case of an isotropic beam with ν = 0.3) and the neutral axis is in the middle. This figure shows two curves: one is associated with the tensile strain due to shear near the edges of the beam, and the other is associated with the tensile strain due to bending in the middle span of the building. The minimum value of $\Delta/L/\varepsilon_{lim}$ between these two curves is a critical value, and it can be used to assess the maximal admissible relative deflection Δ/L. For a given value of the limiting tensile strain (ε_{lim}), the

smallest value of $\Delta/L/\varepsilon_{lim}$ between the two curves indicates whether the failure will occur near the edge section (shear) or near the middle section (bending). It appears that for small values of the ratio L/H, failure will occur near the edge of the building where the maximal tensile strain due to shear first reaches the limiting value ε_{lim}. For greater values of the ratio L/H, failure will occur in the middle section (Figure 2).

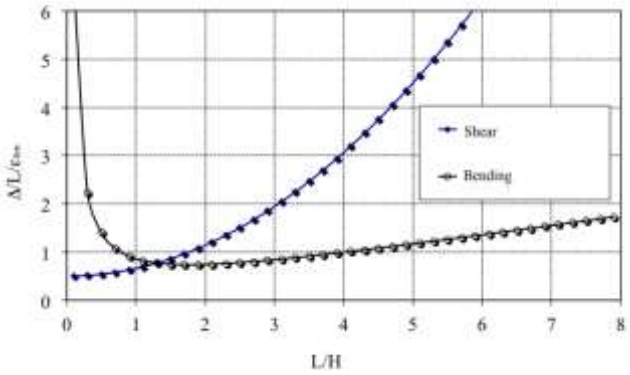

Figure 2. Limiting relationships between $(\Delta/L)/\varepsilon_{lim}$ and L/H.

Comparison of Figure 2 and Table 1 is required to plot abacuses of damage in relation to the deflection ratio and the horizontal strain. Burland developed such abacus for a specific situation: a central point load beam model, with L/H=1 and isotropic properties with E/G = 2.6 (ν = 0.3) (Figure 3).

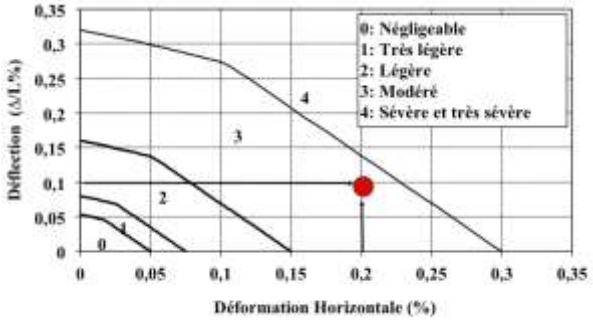

Figure 3. Burland's curves for damage assessment in subsidence zone.

3.2 Determination of an intensity criteria in subsidence areas

The use of an analytical method to develop vulnerability functions raises two difficulties in addition to the definition of the analytical method.

(i) First, the chosen analytical method uses the values of the building induced movement that may be significantly different than the values of the free-field ground movement that would take place without any structure. These differences are the consequence of complex soil-structure interaction phenomena that lead to a transmitted value that may be drastically reduced compared to the free-field ground movement. Nevertheless, the free-field ground movements appear to be relevant for selecting the intensity criteria because they characterize the subsidence, while the transmitted ground movements characterize both the subsidence and the soil-structure interactions. Results of several studies can be used to predict the free-field ground movements (NCB, 1975; Kratzsch, 1983). If Δ_{ground} and ε_{ground} are the free-field ground displacements, two coefficients must be defined to quantify the transmitted movements $\Delta_{structure}$ and $\varepsilon_{structure}$.

$$e_{structure} = K_e \cdot e_{ground} \qquad [6]$$

$$D_{structure} = K_D \cdot D_{ground}$$

The determination of $K\Delta$ and K_ε is difficult, and it depends on the soil and the mechanical characteristics of the building. Boscardin and Cording (1989), and Potts and Addenbrooke (1997) investigated this question for a large range of buildings. For masonry buildings the value of $K\varepsilon$ may vary between 1% and 30% in relation to the building stiffness, and K_Δ may vary between 20% and 70%.

(ii) Secondly, it has been shown that the chosen analytical method is based on two intensity criteria: the building deflection and the transmitted horizontal strain. However, the vulnerability functions are based on the use of unique intensity criteria. Moreover, most empirical methods for building damage assessment in a subsidence area are based on the value of the free-field ground strain (NCB, 1975; Wagner and Schümann, 1991; Yu et al. 1988). Consequently, the free-field horizontal ground strain appears to be the

most efficient choice for the intensity criteria. This choice raises the question of the relationship between the free-field horizontal ground strain and the ground deflection.

According to empirical studies from different countries for different geological contexts and both longwall, and room and pillar mining methods (Karmis et al. 1984;, Orchard and Allen 1965), a relation between the free-field horizontal ground strain ε_{ground} and the ground radius of curvature R_{ground} can be defined according to Equation 2 (Fig. 6).

$$e_{ground} = K_{site}\sqrt{1/R_{ground}} \qquad [7]$$

K_{site} is a coefficient that probably depends on the geological and mining context (mining method, mine geometry, overburden, …) but no study has investigated this point and its determination is mainly based on empirical data.

Moreover, in the case of mining subsidence, the building length is mostly smaller than the subsidence dimensions and the ground curvature may be assumed constant over the building. It is then possible to calculate (beam theory) the geometric relationship between the ground curvature and the ground deflection, using the building length L and considering a circular shape for both the ground and building final curvature (Burland and Wroth, 1974; Burland et al., 1977; Kratzsch, 1983, Eq. 8).

By substituting Equation 8 into Equation 7, the relationship between the ground deflection and the horizontal ground strain is obtained (Eq. 9). Then, by substituting Equation 9 into Equation 7, the relationship between the building deflection and the horizontal structure strain is obtained (Eq. 10).

$$D_{ground} = \frac{L^2}{8R_{ground}} \qquad [8]$$

$$\frac{D_{ground}}{L} = \frac{e^2_{ground}}{8K^2_{site}}.L \qquad [9]$$

$$\frac{D_{Structure}}{L} = \frac{K_D}{K^2_e \cdot K^2_{site}} \cdot \frac{L \cdot e^2_{Structure}}{8} \qquad [10]$$

4 DEVELOPMENT OF VULNERABILITY CURVES

The methodology used to develop the vulnerability and fragility curves is described in precedent section. The free-field horizontal ground strain is chosen as the intensity criteria, and the analytical method is based on the Burland (1995) method. In this study, two masonry building types are investigated, with the same geometric parameters (L, H) taken into consideration. Unreinforced masonry buildings (URM) that are moderately rigid are considered first, and more rigid reinforced masonry buildings (RM) are considered second. Table 2 describes the two building types, where each parameter is variable because of the variability of the buildings within the same type due to real physical and observed differences between the buildings. Moreover, this table also takes into account uncertainties concerning their true characteristics. Length and height are chosen to be representative of the buildings in many mining regions, particularly the Lorraine region.

Table 2. Variability of the parameters for the two building types used in simulating a database of virtual buildings.

	Building			Soil and soil structure interaction coefficients				
Building type	Length [m]	Height [m]	L/H	E/G	ν	K_{site}	K_Δ	K_ε
Unreinforced Masonry (URM)	20-30	7-10	2-4.2	10-15	0.2-0.3	0.1 - 0.2	40 - 70%	10 - 30%
Reinforced Masonry (RM)	20-30	7-10	2-4.2	2-5	0.2-0.3	0.1 - 0.2	20 - 50%	1 à 20%

According to the fourth step of the methodology, the damage is calculated for all 1000 simulated buildings and for different values of the horizontal ground strain. Calculations are performed with Mathematica software (Wolfram, 2007) in which the analytical method is implemented. Because of the parameter variability, not all the buildings suffer the same damage for a given value of horizontal ground strain. Vulnerability curves for a given building type show the relationship between the mean damage and the horizontal ground strain. The mean damage is calculated from Eq. 11.

$$\mu_D(\varepsilon) = \sum_{i=1}^{4} \frac{N(D_i)}{n} \times D_i = \sum_{i=1}^{4} P(D_i) \times D_i \qquad [11]$$

$\mu_D(\varepsilon)$ is the mean damage for the value ε_{ground} of the horizontal ground strain, $N(D_i)$ is the number of buildings in the damage class D_i among the 1000 simulated buildings, and $P(D_i)$ is the percentage of the 1000 buildings with a damage of D_i.
Vulnerability curves may then be modelled in order to obtain a vulnerability function. The tangent hyperbolic function is often used in other fields (Lagomarsino and Giovinazzi 2006), according to Eq.12.

$$\mu_D(\varepsilon) = a[b + Tanh(c \times \varepsilon + d)] \qquad [12]$$

Where $\mu_D(\varepsilon)$ is the mean damage for a value ε_{ground} of the horizontal ground strain, and a, b, c, and d are four coefficients that must be determined for each building type. For example the vulnerability curves for the two building types described in Table 2 are shown in Figure 4. The equations of the fitted curves for these two buildings types are:

For URM type: $\mu_D(\varepsilon)$=2.1(0.89+Tanh(0.5ε-1.43) [13]

For RM type: $\mu_D(\varepsilon)$=2.1(0.88+Tanh(0.38ε-1.42)

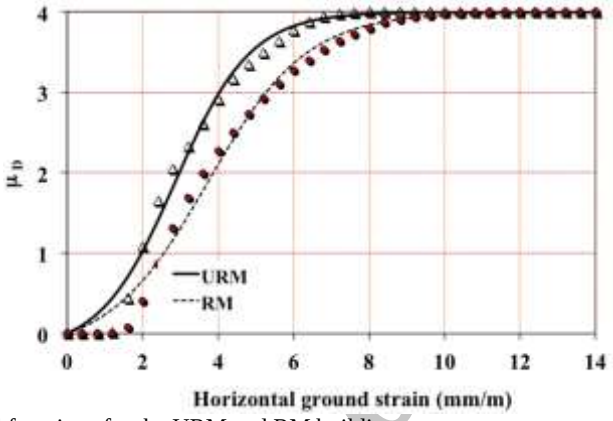

Figure 4. Vulnerability curves and functions for the URM and RM building types.

Comparison of vulnerability curves in Figure 4 shows that for each value of the horizontal ground strain, the mean damage for the reinforced masonry buildings (RM) is less than that for the unreinforced masonry buildings (URM). This is consistent with the fact that the URM buildings are more vulnerable compared to the RM buildings.

5 EFFECT OF SOIL STRUCTURE INTERACTION ON VULNERABILITY FUNCTIONS

A sensitivity analysis was conducted in order to support the selection of values for the K_{site}, K_Δ and K_ε parameters. In this analysis the parameter L/H, E/G and ν are constants (Table 3). The K_Δ and K_ε parameters take values between 0.05 and 1 and the considered K_{site} parameter varies between 0.1 and 0.8.

Figure 5 is used to analyze the influence of K_{site}. It is observed that large values of K_{site} lead to a flattening of vulnerability curves. Moreover, the influence of K_{site} decreases with increase in its value. In other words, the choice of the variability K_{site} (or its range of variation) is particularly important when small values are considered.

Table 3. Parameter values L/H, E/G and ν for the sensitivity analysis of K_{site}, K_Δ and K_ε parameters.

L/H	E/G	ν
2,2- 4,3	10-15	0.2-0.3

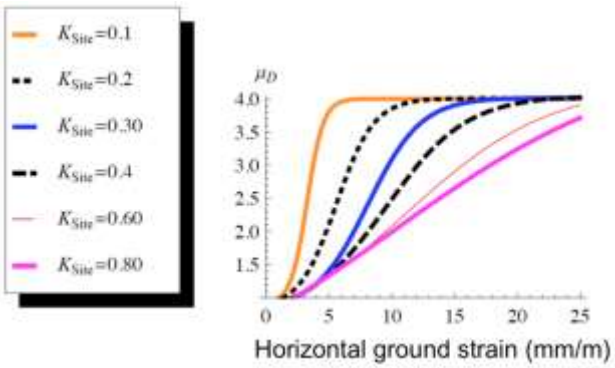

Figure 5. Sensitivity analysis on the K_{site} parameter with K_Δ, K_ε = 0.1 and = 0.2.

Figure 6 is used to analyze the influence of parameter K_Δ. Low values of K_Δ lead to a flattening of the curve (low vulnerability). Figure 7 allows analyzing the influence of the parameter K_ε. It is observed that low values of K_ε lead to a shift of the curve to the right (reduced vulnerability). Sensitivity curves appear identical, whatever the values of K_ε.

Finally, it is observed that the vulnerability curves are more sensitive to values of K_Δ and K_{site}, than to K_ε values.

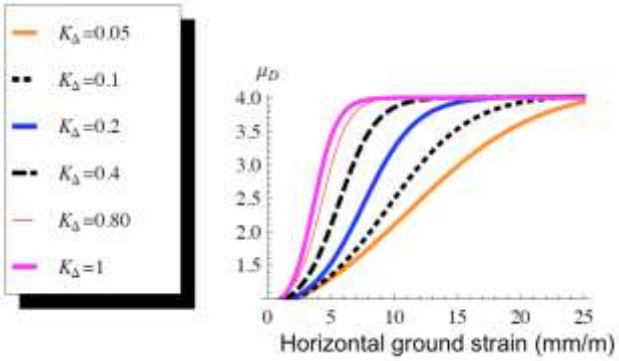

Figure 6. Sensitivity analysis on the K_Δ parameter with K_{site}, K_ε = 0.1 and = 0.2.

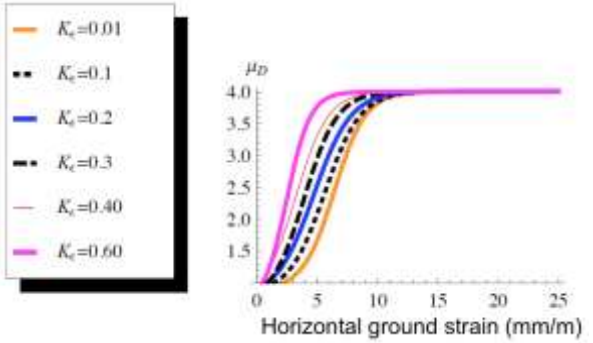

Figure 7. Sensitivity analysis on the K_ε parameter with K_Δ, K_{site} = 0.1 and = 0.2.

6 CONCLUSION

Vulnerability and fragility curves are efficient methods for the assessment of building damage. They also take into account uncertainty in the assessment process. Their use allows the probability to reach or exceed any given damage level for assessment. The Mont Carlo simulation method was used to develop the vulnerability functions with a database of 1000 simulated buildings whose parameters are randomly selected within their possible range of variation for each building type.

A sensibility analysis is done for evaluating the effects of the soil-structure interaction parameters on the vulnerability curve of buildings. It is observed that low values of K_Δ lead to a flattening of the curve (low vulnerability).

For the effects of K_ε parameter, it is observed that low values of K_ε lead to a shift of the curve to the right (reduced vulnerability). Sensitivity curves appear identical, whatever the values of K_ε.

Finally, we can conclude that the vulnerability curves are more sensitive to values of K_Δ and K_{site} than to values K_ε.

REFERENCES

Boone S.J. 1996. Ground-movement related building damage, *J. Geotech. Engng ASCE* 122, No. 11: 886-896.

Boscardin M.D. and Cording E.J. 1989. Building response to excavation – induced settlement, *J. of Geotechnical Engineering*, 115: 1-21.

Burd, H.J. Houlsby, G.T. Augarde, C. E. 2000. Modelling tunnelling-induced settlement of masonry buildings, *Proc. Instn Civ. Engrs Geotech. Eng*, 143, 17-29.

Burland, J.B. Wroth, C.P. 1974. Settlement of buildings and associated damage. *Conf. settlement of structures*, 611-654.

Burland, J.B. Broms, B.B. and De Mello, V.F.B. 1977. Behaviour of foundations and structures, *9th Int.conf. on soil mechanics and foundations engineering*, Tokyo 2: 495-546.

Burland, J.B. 1995. Assessment of risk of damage to building due to tunneling and excavation, *Proc. 1st Int. Conf. Earthquake Geotechnical Engineering*, Ishihara(ed.), Balkema, 1189-1201.

Carlos, E. Ventura, W.D. Liam F. Onur, T. Blanquera, A. Rezai, M. 2005. Regional seismic risk in British Colombia-Classification of buildings and development of damage probability functions. *Canadian journal civil engineering* 32: 372-387.

Coulthard, M.A. Dutton, A.J. 1998. Numerical modeling of subsidence induced by underground coal mining, *The 29th U.S. Symposium on Rock Mechanics (USRMS)*, Minneapolis, MN.

Franzius, J.N., Potts, D.M. and Burland, J.B. 2006. The response of surface structures to tunnel construction, *Proceedings of the institution of civil engineers*, 159: 3-17.

Finno, R.J. Voss, F.T. Rossow, E. Tanner, B. 2005. Evaluating Damage Potential in Buildings Affected by Excavations, *Journal of Geotechnical and Geoenvironmental Engineering* 131, No. 10: 1199-1210.

Karmis, M. Triplett, T. and Schilizzi P. 1984. Recent developments in subsidence prediction and control for the eastern U.S. coalfield, *25 th. Symp. on rock mechanics*, 713-913.

Kratzsch, H. 1983. Mining Subsidence Engineering, Springer-Verlag.

Lagomarsino, S. Giovinazzi, S. 2006. Macroseismic and mechanical models for the vulnerability and damage assessment of current buildings, *Earthquake Engineering*, 4: 415–443.

Melis, A. Medina, L. and Rodríguez, J.M. 2002. Prediction and analysis of subsidence induced by shield tunneling in the Madrid Metro extension. *Can. Geotech. J.* 39(6): 1273–1287.

National Coal Board. 1975. Subsidence engineering handbook. chapter 6: 45-56.

Orchard, R.J. Allen, W.S. 1965. Ground curvature due to coal mining, *Chartered Surveyor*, 97: 622-631.

Potts, D.M. Addenbrooke, T.I. 1997. A structure's influence on tunnelling-induced ground movements, *Proc. Incln. Civ. Engng*, 125: 109 - 125.

Saeidi, A. Deck, O. Verdel, T. 2009. Development of vulnerability functions in subsidence regions from empirical methods, *Engineering structure Journal*, doi:10.1016/j.engstruct.2009.04.010.

Saeidi, A. Deck O. and Verdel, T. 2013. Comparison of Building Damage Assessment Methods for Risk Analysis in Mining Subsidence Regions, *Geotechnical and Geological Engineering, 31*(4): 1073-1088. doi: 10.1007/s10706-013-9633-7

Skempton, A.W. MacDonald, D.H. 1956. Allowable settlement of building, *Proc. INSTN. Civ. Engrs*, 3, 5: 727-768.

Son, M. and Cording, E.J. 2005. Estimation of building damage due to excavation-induced ground movements. *Journal of Geotechnical and Geoenvironmental Engineering*, 131, 2: 162-177.

Timoshenko, S. 1957. Strength of material-part I, D van Nostrand Co, Inc. London.

Wagner, H. Schümann, E.H.R. 1991. Surface effect of total coal seam extractions by underground mining methods. *J.S.Afr.Inst.Min.Metal*, 91: 221-231.

Wolfram, S. 2007. Mathematica software version 6, *Wolfram Research*, Inc., USA.

Yu, Z. Karmis, M. Jarosz, A. Haycocks C., 1988, Development of damage criteria for buildings affected by mining subsidence, *6th annual workshop generic mineral technology centre mine system design and ground control*, 83-92.